MOLECULAR AND CELLULAR BIOLOGY, Sept. 2006, p. 6623–6632 Vol. 26, No. 17
0270-7306/06/$08.00+0 doi:10.1128/MCB.02460-05

# Cytohesin Binder and Regulator (Cybr) Is Not Essential for T- and Dendritic-Cell Activation and Differentiation†

Wendy T. Watford,[1]* Denise Li,[1] Davide Agnello,[1] Lydia Durant,[1] Kunihiro Yamaoka,[1] Zheng Ju Yao,[1] Hyun-Jong Ahn,[1] Tammy P. Cheng,[1] Sigrun R. Hofmann,[1] Tiziana Cogliati,[2]‡ Amy Chen,[3] Bruce D. Hissong,[1] Matthew R. Husa,[1] Pamela Schwartzberg,[3] John J. O'Shea,[1] and Massimo Gadina[1]§

*Molecular Immunology and Inflammation Branch, NIAMS,[1] Genetics Department, NCI,[2] and NHGRI,[3] National Institutes of Health, Bethesda, Maryland 20892*

Received 23 December 2005/Returned for modification 7 March 2006/Accepted 22 June 2006

**Cybr (also known as Cytip, CASP, and PSCDBP) is an interleukin-12-induced gene expressed exclusively in hematopoietic cells and tissues that associates with Arf guanine nucleotide exchange factors known as cytohesins. Cybr levels are dynamically regulated during T-cell development in the thymus and upon activation of peripheral T cells. In addition, Cybr is induced in activated dendritic cells and has been reported to regulate dendritic cell (DC)-T-cell adhesion. Here we report the generation and characterization of Cybr-deficient mice. Despite the selective expression in hematopoietic cells, there was no intrinsic defect in T- or B-cell development or function in Cybr-deficient mice. The adoptive transfer of Cybr-deficient DCs showed that they migrated efficiently and stimulated proliferation and cytokine production by T cells in vivo. However, competitive stem cell repopulation experiments showed a defect in the abilities of Cybr-deficient T cells to develop in the presence of wild-type precursors. These data suggest that Cybr is not absolutely required for hematopoietic cell development or function, but stem cells lacking Cybr are at a developmental disadvantage compared to wild-type cells. Collectively, these data demonstrate that despite its selective expression in hematopoietic cells, the role of Cybr is limited or largely redundant. Previous in vitro studies using overexpression or short interfering RNA inhibition of the levels of Cybr protein appear to have overestimated its immunological role.**

By using microarray analysis, the cytohesin binder and regulator (Cybr, Cytip, CASP, or PSCDBP) was originally identified as an interleukin-12 (IL-12)-inducible gene in T cells (18, 19). Cybr protein is predicted to contain two protein interaction domains: a PDZ domain and a coiled-coil domain. We and others have shown that Cybr interacts with members of the cytohesin family of proteins and regulates their activity, as the name implies (1, 12, 19). A structurally related protein designated tamalin also interacts with cytohesins (8, 9); however, unlike Cybr, which is expressed primarily in hematopoietic cells, tamalin is expressed almost exclusively in neuronal tissues. Tamalin has been reported to function as a scaffold protein involved in intracellular trafficking and to regulate cell surface expression of group 1 metabotropic glutamate receptors in neuronal cells (8, 9). Together, Cybr and tamalin may constitute a new small family of molecular scaffold proteins that appear to regulate cytohesin function.

Cytohesins are a group of guanine nucleotide exchange factors (GEFs) that control the activities of ADP-ribosylation factors (Arfs), small GTP binding proteins that regulate vesicular transport pathways and organization of the actin cytoskeleton (reviewed in reference 17). Regulated binding and hydrolysis of GTP by Arfs is critical for their activation and function, but Arfs lack intrinsic nucleotide exchange activity. Instead, accessory proteins, such as cytohesins and Arf-GAPs, provide these functions. There are seven known cytohesins: cytohesin-1 (B2-1), cytohesin-2 (Arf nucleotide binding-site opener), cytohesin-3 (general receptor for phosphoinositides [GRP1]), cytohesin-4, cytohesin-5 (EFA6), cytohesin-6 (Tic), and cytohesin-7 (HCAA67). The cytohesins are defined by characteristic protein domains, including a Sec7 homology domain required for GEF activity, a coiled-coil region, and a pleckstrin homology domain for membrane localization through binding to phosphatidylinositols (7). We have previously shown that Cybr interacts with cytohesin-1 and that this interaction occurs homotypically between the coiled-coil domains of the two proteins (19). Through this interaction, Cybr is able to regulate cytohesin-1's GEF activity for Arf1 (19). Moreover, Cybr has also been shown to be recruited from the peri-Golgi compartment to membrane ruffles of epidermal growth factor-stimulated cells in a cytohesin-dependent manner (12) but the physiological consequences of this recruitment are not fully understood.

One putative function of cytohesins is to regulate cell adhesion. Based on overexpression studies, cytohesin-1 has been reported to modulate integrin-mediated cell adhesion through association with the cytoplasmic domain of the β2 subunit of the β2 integrin family member LFA-1 (4). Through its interaction with cytohesin-1, Cybr has also been reported to play a role in cellular adhesion. An overexpression of Cybr results in

* Corresponding author. Mailing address: LCBS-MIIB-NIAMS-NIH, Bldg. 10, Room 9N256, MSC-1820, 10 Center Dr., Bethesda, MD 20892-1820. Phone: (301) 496-2541. Fax: (301) 402-0012. E-mail: watfordw@mail.nih.gov.

† Supplemental material for this article may be found at http://mcb.asm.org/.

‡ Present address: Department of Ophthalmology, Queen's University of Belfast, Belfast, United Kingdom.

§ Present address: Centre for Cancer Research and Cell Biology, Queen's University of Belfast, Belfast, United Kingdom.

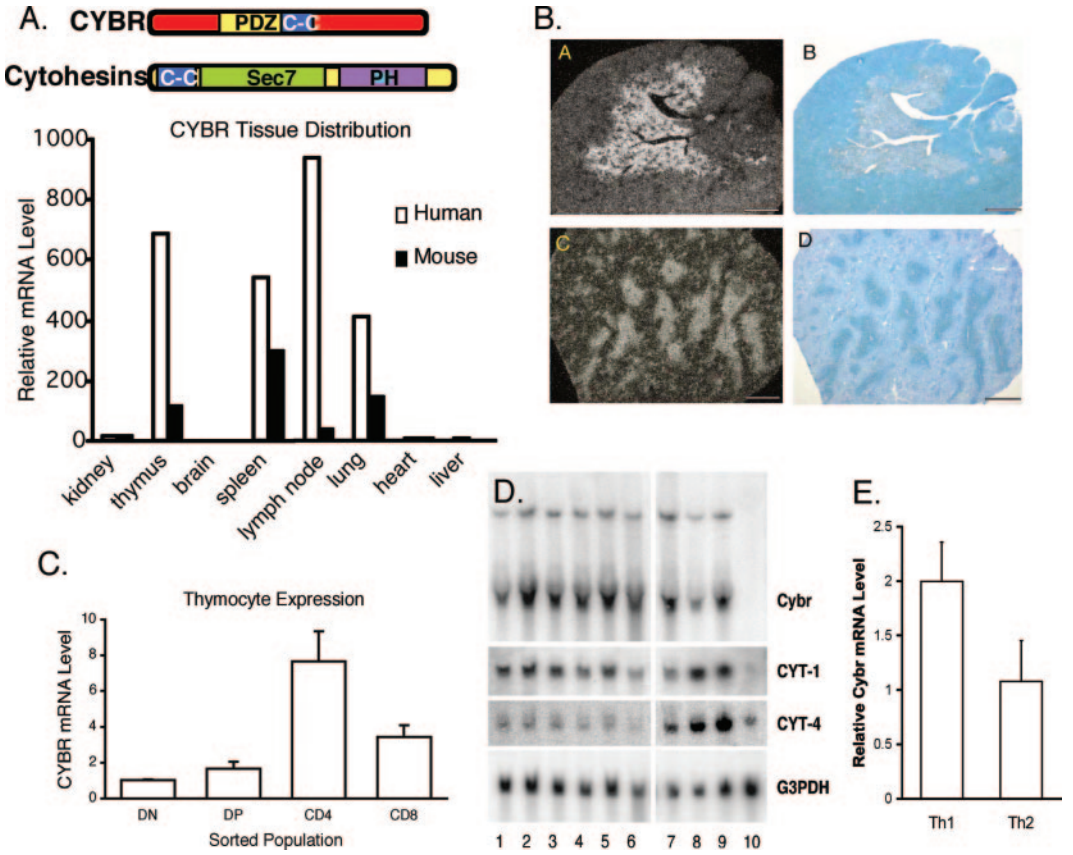


FIG. 1. Cybr is expressed in hematopoietic tissues and regulated by cytokine stimulation. (A) Cybr expression was analyzed in RNA isolated from various mouse and human tissues by real-time PCR. (B) Dark field (A and C) and bright field (B and D) microphotographs of cryosections from adult mouse thymus (A and B) and spleen (C and D) were obtained after in situ hybridization with $^{35}$S-labeled antisense murine Cybr probes. Cybr expression is localized to the thymic medulla (A) and spleen white pulp (C). Counterstaining (B and D) was performed with 0.5% methyl green. (C) Mouse thymocyte populations were FACS sorted and analyzed for Cybr expression during thymic development by real-time PCR. Error bars indicate standard deviations. DN, double negative; DP, double positive. (D) Human peripheral blood mononuclear cells and MoDCs were stimulated with cytokine and analyzed for Cybr expression by Northern blotting. Peripheral blood mononuclear cells were cultured with media alone (lane 1) or stimulated with IL-2, IL-7, IL-12, IL-15, or IL-12 and IL-18 (lanes 2 to 6). Monocytes (lane 7), immature MoDCs (lane 8), or MoDCs matured with TNF-α treatment (lane 9) were also analyzed for Cybr expression. Unlike primary monocytes, the monocytic cell line THP-1 did not express Cybr (lane 10). (E) Cybr expression was analyzed in in vitro-polarized Th1 and Th2 cells by real-time PCR. Error bars indicate standard deviations.

the sequestration of cytohesin-1 in the cytoplasm away from membrane-associated LFA-1. In this way, Cybr is proposed to negatively regulate lymphocyte adhesion (1). Recently, the silencing of Cybr by short interfering RNA (siRNA) in human monocyte-derived dendritic cells (MoDCs) was reported to inhibit the dissolution of dendritic cell (DC)–T-cell conjugates, also implying a role in hematopoietic cell adhesion (5).

Cybr mRNA levels are regulated during T-cell activation and differentiation (19), but the precise function of Cybr in T cells is unknown. Two microarray studies have identified Cybr as a gene that is differentially regulated during positive selection in the thymus (6, 13). Additionally, we have shown that Cybr mRNA levels are increased upon IL-12 stimulation in T cells (19). These data suggest potential roles for Cybr and the Arf/cytohesin pathway during T-cell development. Through its interactions with the cytohesins, Cybr could be predicted to regulate actin cytoskeletal rearrangements, such as immunological synapse formation, that take place during antigen recognition by T cells. Alternatively, Cybr may function later to regulate cellular activation and/or cytokine secretion by lymphocytes.

Herein, we address the in vivo role(s) of Cybr in hematopoietic cells by generating Cybr-deficient mice. To our surprise, given the published reports of the effects of Cybr on T- and dendritic-cell functions, Cybr protein was not required for normal immune cell development or functions in mice. However, in a competitive repopulation setting, Cybr-deficient stem cells were inefficient at competing with wild-type cells in the generation of hematopoietic lineages. These data suggest that while Cybr is not absolutely required for lymphocyte development, function, or trafficking in the periphery, stem cells lacking Cybr are at a minor developmental disadvantage relative to wild-type cells. The molecular mechanisms leading to this impairment are still unknown but do not seem to include defective chemotactic responses and/or trafficking capability based on the migration of mature T and dendritic cells. These findings demonstrate that despite its selective expression in hematopoietic cells, the role of Cybr in immune cell function is nonessential, possibly due to functional redundancy with other proteins.

## MATERIALS AND METHODS

**Mice.** Mice were bred under specific-pathogen-free conditions at the National Institutes of Health (NIH) or at Taconic Farms (Germantown, NY) and were

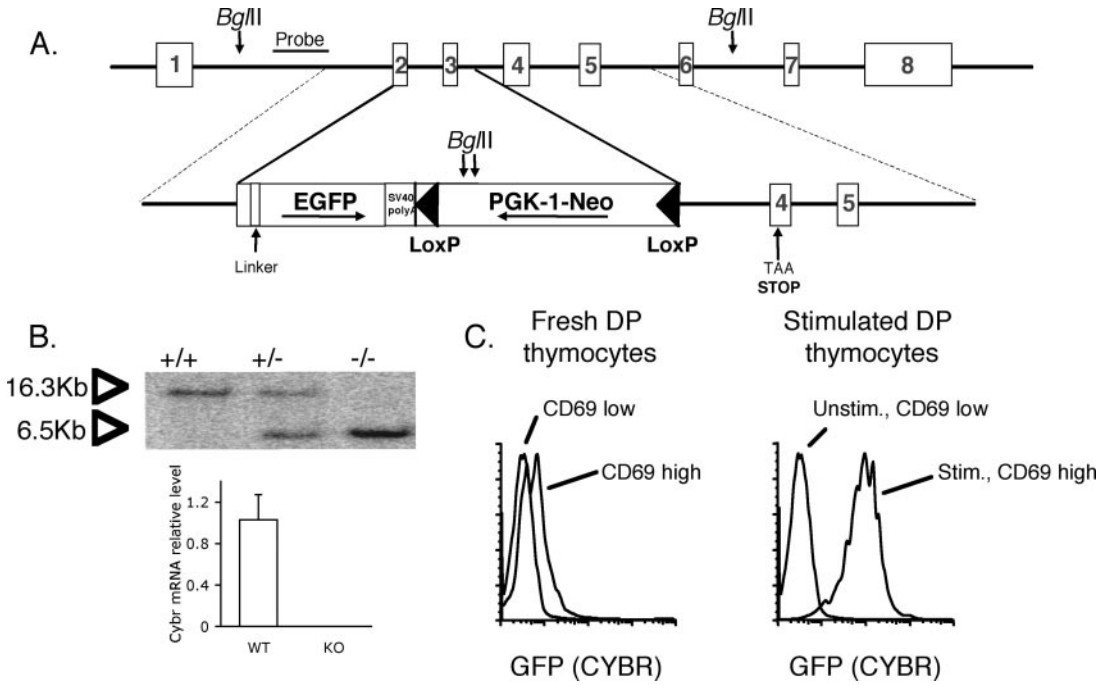


FIG. 2. Generation of Cybr knockout, GFP knockin mice. (A) The endogenous Cybr locus (upper panel) and targeting vector (lower panel) are illustrated. Part of exon 2 and the entire third exon are deleted, and a stop codon is engineered in exon 4 of the recombined allele. In addition, EGFP is expressed as a fusion protein with the N-terminal part of Cybr encoded by exon 1 and part of exon 2 under the endogenous Cybr promoter. Panel B, upper panel, shows that homologous recombination was confirmed by Southern blotting. Lack of Cybr mRNA expression was confirmed in lymphocytes from homozygous mice by real-time PCR using primers and probe that amplify at the exon 5/exon 6 boundary outside of the targeted region of the gene. Panel B, lower panel, shows that lymphocytes were stimulated in vitro under Th1-polarizing conditions for optimal Cybr expression. Error bars indicate standard deviations. (C) Cybr promoter activity was tracked using EGFP expression by flow cytometry in double-positive (DP) thymocytes that were either unstimulated (unstim.) or stimulated (stim.) with anti-CD3 and anti-CD28. Activated thymocytes expressing CD69 had high levels of Cybr promoter activity, as measured by GFP expression.

used between 6 and 12 weeks of age in accordance with institutional animal care and use guidelines.

**Reagents.** Murine cells were cultured in RPMI 1640 containing 10% heat-inactivated fetal calf serum, 2 mM L-glutamine, 1 mM sodium pyruvate, 10 mM HEPES, 50 μM β-mercaptoethanol, 100 U/ml penicillin, and 100 μg/ml streptomycin. Murine IL-4 and IL-12 were purchased from R&D Systems (Minneapolis, MN), and human IL-2 was provided by C. Reynolds (NCI, Frederick, MD). Antibodies against murine IL-4, IL-12, CD3, and CD28 were purchased from Pharmingen (San Diego, CA).

**Gene targeting of murine Cybr.** The targeting construct was electroporated into the 129/SvEv mouse embryonic stem (ES) cell line TC1. Homologous recombination between the targeting construct and the endogenous Cybr locus resulted in the exchange of part of exons 2 and 3 with the sequence encoding enhanced green fluorescent protein (EGFP) in frame with the N-terminal part of Cybr, followed by the simian virus 40 poly(A)$^+$ tail and the LoxP-flanked PGK-1-Neo cassette inserted in the opposite orientation. ES cells resistant to G418 selection were screened by Southern blotting to detect clones that had undergone recombination. The external probe used to screen colonies was synthesized by PCR using BAC-81 as a template. The primers were 5′-ATA ACC ATG CCA TGC CCT AGG GGT-3′ and 5′-CTC TCC TGC TGT CTC TGA AGA CAG-3′. The digestion of genomic DNA with BgIII and hybridization with this probe generated a 16.3-kb band, whereas an additional 6.5-kb band appeared when homologous recombination had occurred. Recombined ES cell clones were used for microinjection into C57BL/6J blastocysts that were implanted into pseudopregnant NIH Swiss Webster female mice. The same screening strategy identified four independent chimeras that were bred to wild-type C57BL/6 mice to obtain *Cybr*$^{+/-}$ mice. Heterozygous mice were backcrossed from six to nine generations to C57BL/6 mice, at which point they were intercrossed to obtain *Cybr*$^{-/-}$ and *Cybr*$^{+/+}$ littermate controls. The functionality of the knocked-in *eGFP* gene was assessed by flow cytometry.

**Gene expression.** mRNA was harvested from cells by using an RNeasy kit (QIAGEN). For Northern blot analysis, 10 μg of total RNA was separated on 1% agarose-glyoxal gel, transferred to nylon membranes, and hybridized to a radiolabeled full-length murine Cybr, cytohesin-1, cytohesin-4, or G3PDH probe (Clontech). First-strand cDNA synthesis and real-time PCR were performed as described previously using primer and probe sets from Applied Biosystems (Foster City, CA) (15). In addition, cryosections (16 μm) from adult mouse thymus and spleen were hybridized in situ with $^{35}$S-labeled sense and antisense murine Cybr probes as previously described (2) and counterstained with 0.5% methyl green.

**Antibodies and flow cytometry.** Antibodies labeled with fluorescein isothiocyanate, phycoerythrin, peridinin chlorophyll protein, allophycocyanin, and biotin were purchased from BD Pharmingen. Cells were stained for surface expression of the following markers: CD4, CD8, CD25, CD44, B220, and CD19. Flow cytometry was performed on a FACSCalibur (Becton Dickinson, Franklin Lakes, NJ) using CellQuest software and was analyzed with FlowJo software (Tree Star, Ashland, OR). Live cells were gated according to their forward-scatter and side-scatter profiles. Cell sorting to obtain pure populations of CD4$^+$, CD8$^+$, CD4$^+$ CD8$^+$, and CD4$^-$ CD8$^-$ cells was performed using a high-speed sorter (MoFlo; DakoCytomation, Fort Collins, CO).

**T-cell functional assays.** For proliferation and cytokine production studies, CD3$^+$ or naïve CD4$^+$ T cells were isolated from splenocytes using murine T-cell enrichment columns (R&D Systems). Cells ($1 \times 10^6$/200 μl) were plated on wells precoated with anti-CD3 and -CD28. Supernatants were collected at 24 h after plating and analyzed for cytokine production by cytokine bead array (BD Pharmingen). Plates were pulsed at 24 h with 1 μCi [$^3$H]thymidine (Amersham) overnight and harvested on a 96-well plate harvester, and isotope incorporation was determined by scintillation counting.

T-helper-cell polarization was performed by culturing naïve CD4$^+$ T cells on 24-well tissue culture plates precoated with anti-CD3 and anti-CD28. For Th1 polarization, cells were stimulated with 20 μg/ml anti-IL-4 plus 20 ng/ml IL-12 and 50 U/ml IL-2. For Th2 polarization, cells were treated with 20 μg/ml anti-IL-12 plus 20 ng/ml IL-4 and 50 U/ml IL-2. After 3 days, IL-2 with either IL-12 (Th1) or IL-4 (Th2) was added to expand the cells. On day 7, cells were restimulated with plate-bound anti-CD3, and polarization was confirmed by measuring IL-4 and gamma interferon (IFN-γ) mRNA levels by real-time PCR and intra-

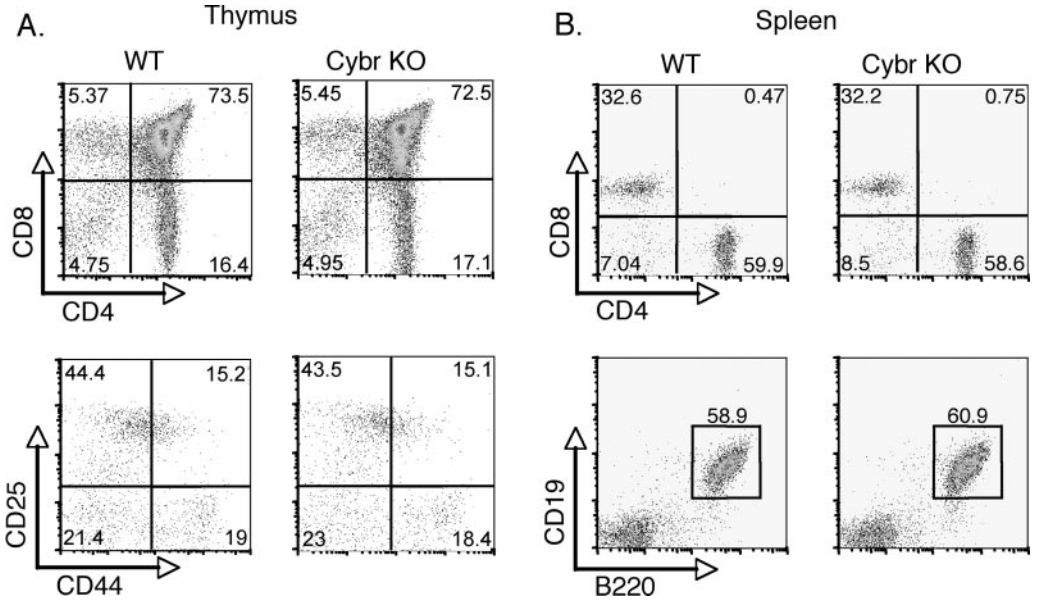


FIG. 3. Normal lymphoid development in Cybr-deficient mice. Lymphocyte populations in thymus or spleen were analyzed by flow cytometry. (A) Thymic CD4 and CD8 single- and double-positive populations (upper panels) as well as double-negative populations DN1 to 4 (as defined by CD25 and CD44 staining) (lower panels) are shown. (B) Spleen CD4 and CD8 T-cell populations (upper panels) and $CD19^+$ B cells (lower panels) were also analyzed. WT, wild type; KO, knockout.

cellular cytokine staining using a fixation and permeabilization solution kit with BD GolgiPlug (Pharmingen).

To measure intracellular calcium mobilization, purified $CD3^+$ T cells ($4 \times 10^6$/ml) were labeled with 1.7 μM Indo (Molecular Probes, Eugene, OR) for 30 min at 37°C in Hanks balanced salt solution containing 0.5% bovine serum albumin. Four million cells were then incubated with biotinylated anti-CD3 (Pharmingen) for 30 min on ice. Cells were washed with a calcium-containing buffer and incubated in a 37°C water bath for 2 min, and baseline data were acquired for 1 min. Cells were then treated with 50 μl streptavidin (20 ng/ml) to cross-link their T-cell receptors (TCRs), and data were collected for an additional four min. As a positive control, cells were then treated with 50 μl ionomycin (20 ng/ml) to induce maximal calcium flux and data were collected for an additional 3 min.

Mature T-cell trafficking in vivo was performed by injecting purified $CD45.2^+$ $CD3^+$ T cells intravenously into $CD45.1^+$ congenic recipient mice and measuring the absolute number of migrated cells 20 h later by flow cytometry. In addition, in vitro T-cell chemotaxis was performed using 96-well chemotaxis plates (5-mm-pore-size membrane; Neuro Probe, Inc., Gaithersburg, MD) as described previously (14).

**Analysis of dendritic cells and macrophages.** $CD11c^+$ dendritic cells from wild-type or Cybr-deficient $CD45.2^+$ mice were generated as described previously by culturing bone marrow in granulocyte-macrophage colony-stimulating factor and IL-4 (20). In vivo migration of bone marrow-derived dendritic cells (BMDCs) was investigated by preincubating $CD45.2^+$ BMDCs with 1 μg/ml lipopolysaccharide (LPS) plus 10 ng/ml IFN-γ for 2 h before injecting them into congenic $CD45.1^+$ recipient mice. One million BMDCs were injected into each footpad, and draining lymph nodes were isolated 24 h later. Cells were purified and stained with phycoerythrin-labeled anti-CD45.2 and allophycocyanin-labeled anti-CD11c to detect the appearance of the donor-derived dendritic cells in the draining lymph node.

To examine the ability of wild-type or Cybr-deficient BMDCs to present antigen to T cells in vivo, we performed adoptive transfer experiments as previously described (20). Briefly, $CD4^+$ T cells from OT-II TCR transgenic mice ($CD45.2^+$) were isolated from peripheral lymph nodes and labeled with carboxyfluorescein diacetate succinimidyl ester (CFSE) (Molecular Probes). Three million labeled cells were injected intravenously into tail veins of C57BL/6 $CD45.1^+$ congenic mice. Concomitantly, BMDCs from $Cybr^{-/-}$ and wild-type mice ($1 \times 10^6$; $CD45.2^+$) were pulsed with $OVA_{329\text{-}339}$ peptide (Research Services Branch, NIAID, NIH) in the presence of LPS plus IFN-γ and injected into fore footpads of the mice that had received the T cells. Three and a half days later, axillary lymph nodes cells were isolated and analyzed for donor T-cell proliferation and cytokine production.

The recruitment of peritoneal macrophages was assessed by injecting mice intraperitoneally with 1 ml of 3% thioglycolate solution. Twenty-four hours later, peritoneal exudate cells were recovered by peritoneal lavage with phosphate-buffered saline containing 0.2 mM EDTA and counted using a hemacytometer.

To analyze phagocytic capacity, thioglycolate-elicited peritoneal macrophages were isolated and incubated with *Escherichia coli* or *Staphylococcus aureus* bacteria labeled with Alexa Fluor (Invitrogen) in phosphate-buffered saline containing 0.1% bovine serum albumin and 1 mM $CaCl_2$ in the presence or absence of 10% serum for 45 min at 37°C. Cells were washed, fixed with 1% formaldehyde, and analyzed by flow cytometry for cell-associated bacteria.

For the assessment of in vivo responsiveness to LPS, mice were injected intraperitoneally with 100 μg of LPS from *Salmonella enterica* serovar Minnesota (Sigma). Blood was collected from the tail vein at 0, 0.5, 1, 2, 4, 8, and 24 h, and serum cytokine levels were determined by cytometric bead array (mouse inflammation cytometric bead array kit; BD Pharmingen).

**Bone marrow competitive repopulation.** Murine bone marrow was isolated from adult male femurs and tibias and depleted of red blood cells by a brief treatment with ACK lysing buffer (Quality Biological, Inc., Gaithersburg, MD). Stem cells were purified using double depletion of lineage marker-positive cells followed by positive selection using anti-CD117 microbeads (Miltenyi Biotec, Auburn, CA). Three million purified stem cells from $CD45.2^+$ wild-type or Cybr knockout mice were injected alone or as a 1:1 mixture with wild-type $CD45.1^+$ stem cells into the lateral tail veins of irradiated (900 rad) $rag2^{-/-}$ recipient mice. After 8 weeks, thymi, lymph nodes, and spleens were harvested and cell populations were analyzed for CD45.1/2 expression by flow cytometry.

## RESULTS

**Cybr is expressed in hematopoietic tissues and regulated by cytokine stimulation.** We and others originally identified Cybr as an IL-12-inducible gene using microarray analysis of human peripheral blood leukocytes (18, 19). To determine whether the Cybr expression pattern seen in human cells was recapitulated in the mouse, we analyzed murine and human tissues by real-time PCR for Cybr expression. We found that Cybr message levels were highest in thymus, spleen, lymph node, and

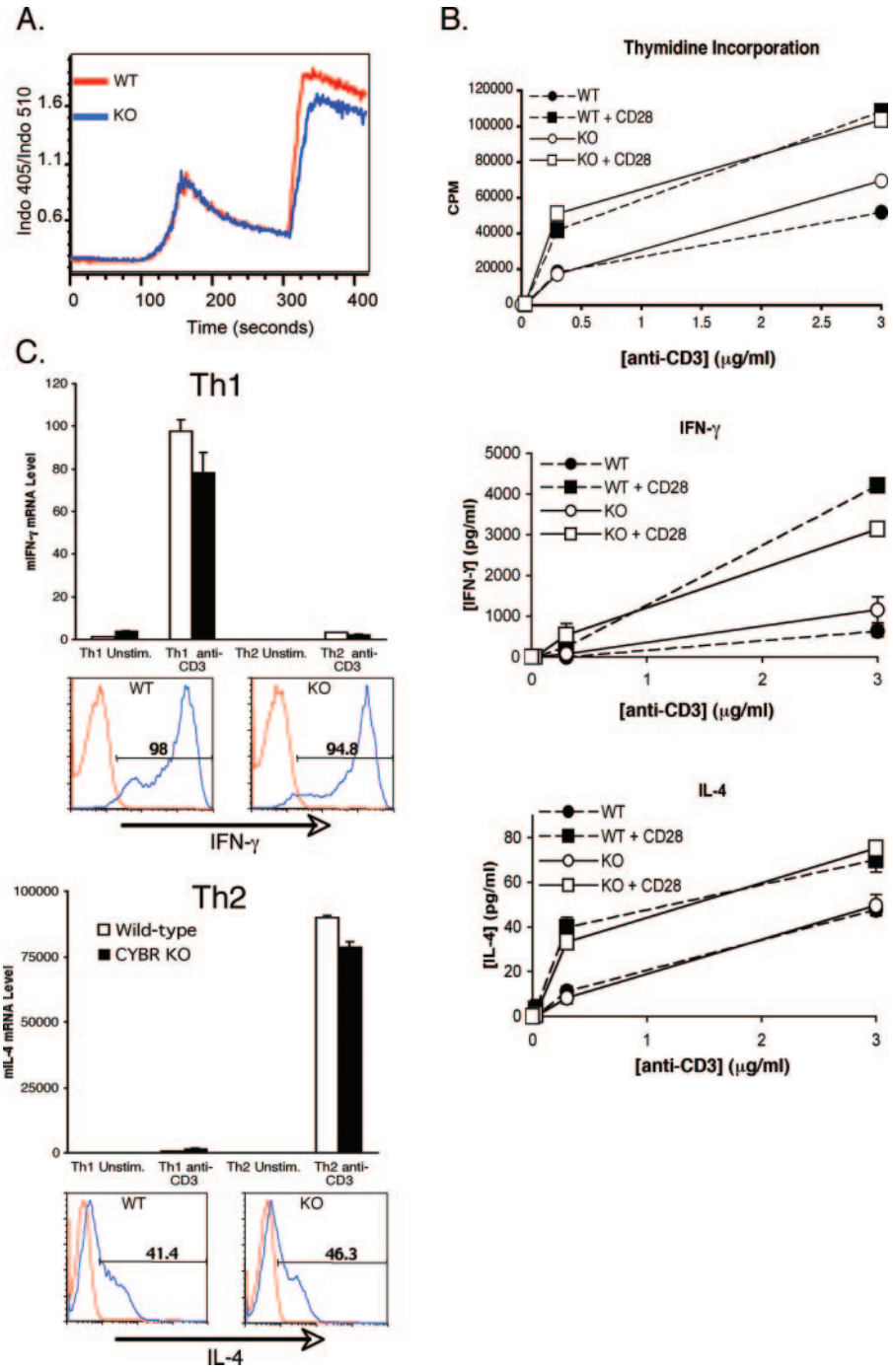


FIG. 4. T-cell functions in Cybr-deficient mice. (A) CD3$^+$ T cells were purified from spleen, and TCR-induced calcium mobilization in response to CD3 cross-linking (at 60 s) or ionomycin (at 300 s) was measured by flow cytometry in cells that had been loaded with the calcium-sensitive dye Indo. (B) CD4$^+$ T cells were analyzed for their abilities to proliferate and produce cytokines in response to stimulation through CD3 in the presence or absence of CD28 costimulation. Proliferation was measured by incorporation of [$^3$H]thymidine. Cytokine production was measured in 24-h cell culture supernatants by cytometric bead array (BD Pharmingen). (C) Wild-type or Cybr-deficient naive CD4$^+$ T cells were polarized under Th1 or Th2 conditions and assayed for the ability to secrete IFN-γ or IL-4, respectively. IFN-γ mRNA (mIFN-γ) or IL-4 mRNA (mIL-4) levels were determined by real-time PCR with or without a 4-h restimulation with plate-bound anti-CD3 (upper panels). Lower panels show intracellular cytokine staining on polarized cells after restimulation with anti-CD3. Error bars indicate standard deviations. WT, wild type; KO, knockout; unstim., unstimulated; stim.; stimulated.

lung in both species, suggesting that Cybr might have a conserved function in hematopoietic cells (Fig. 1A).

Cybr has also been reported to be up-regulated during positive selection of T cells in the thymus (6, 13). Accordingly, in situ hybridization of murine organs showed that Cybr expression was restricted to the thymic medulla, a region that contains predominantly CD4$^+$ and CD8$^+$ single-positive thymocytes. Similarly, splenic white pulp areas rich in mature

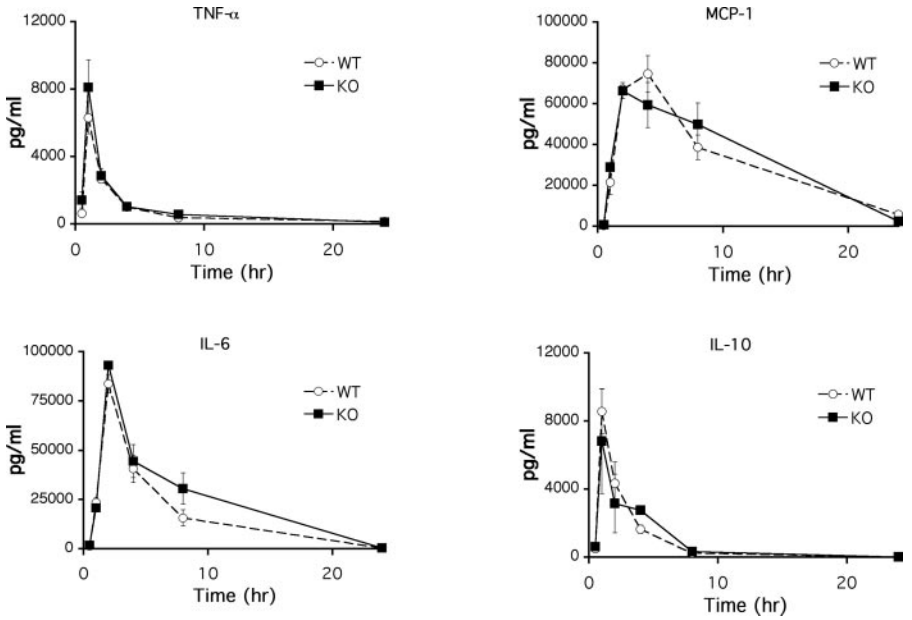


FIG. 5. *Cybr*$^{-/-}$ mice respond normally to LPS challenge. Mice were injected intraperitoneally with 100 μg of LPS from *Salmonella enterica* serovar Minnesota. Blood was collected from the tail vein at 0, 0.5, 1, 2, 4, 8, and 24 h, and serum cytokine levels for TNF-α, monocyte chemoattractant protein 1, IL-6, and IL-10 were determined by cytometric bead array (mouse inflammation cytometric bead array kit; BD Pharmingen). Error bars indicate standard deviations. WT, wild type; KO, knockout.

lymphocytes also exhibited preferential Cybr expression (Fig. 1B). To determine whether Cybr is regulated during thymic development, we isolated pure populations of CD4$^+$ and CD8$^+$ thymocytes and analyzed them for Cybr expression by real-time PCR. We found that Cybr expression was low in double-negative and double-positive populations and that it increased during maturation to the CD4$^+$ or CD8$^+$ single-positive stage (Fig. 1C).

While microarray studies indicated that Cybr was an IL-12-inducible gene, we sought to examine its specificity. Further analysis of human peripheral blood lymphocytes showed that Cybr was induced by a variety of cytokines, including IL-2, IL-7, and IL-15 (Fig. 1D, lanes 2, 3, and 5). Cybr message levels are also high in monocytes and monocyte-derived DCs after maturation with tumor necrosis factor alpha (TNF-α), as previously described (19). No Cybr expression was found in the THP-1 monocyte cell line (Fig. 1D, lane 10). We and others have shown that Cybr interacts with cytohesin-1 (1, 12, 19). Therefore, we also examined cytohesin regulation in response to cytokine stimulation. Neither cytohesin-1 nor cytohesin-4 was inducibly regulated by cytokine stimulation in human peripheral blood lymphocytes (Fig. 1D, lanes 1 to 6). However, both cytohesin-1 and cytohesin-4 were upregulated in monocyte-derived DCs relative to monocytes (Fig. 1D, lanes 7 to 9). Given that Cybr is induced by IL-12 in mouse and human cells and that Cybr is a Th1-associated gene in human cells (19), we analyzed Cybr expression in polarized murine Th1 and Th2 cells by real-time PCR. As in human T cells, Cybr expression was higher in Th1 cells than in Th2 cells, consistent with its induction by IL-12 (Fig. 1E).

**Cybr-deficient mice have normal lymphocyte development.** To better define the in vivo functions of Cybr, we generated Cybr-deficient mice. The targeting construct is depicted in Fig. 2A. The recombined locus lacks the majority of exon 2 and the entire third exon and has a stop codon engineered within exon 4 to prohibit the generation of a transcript through alternative splicing. Chimeric mice were bred to generate heterozygotes that were subsequently intercrossed to generate homozygous knockout mice. Recombination of the locus was confirmed by Southern blotting, and the absence of Cybr mRNA expression was confirmed by real-time PCR in lymphocytes from homozygous mice after stimulation under Th1-polarizing conditions, in which Cybr is normally highly induced (Fig. 2B). Cybr-deficient mice were born in normal Mendelian frequencies and were viable with no obvious phenotypic or pathological alterations. Complete blood counts showed no significant difference in lymphocyte counts in peripheral blood (data not shown).

The targeted allele expresses EGFP as a fusion protein with the N-terminal part of Cybr that is encoded by exon 1 and part of exon 2. Since green fluorescent protein (GFP) expression is under the regulation of the endogenous Cybr promoter, this provided a tool for monitoring Cybr promoter activity in vivo. Using heterozygous mice, Cybr promoter activity was tracked using the GFP reporter knocked into the Cybr locus. CD69 expression was used as an activation marker because its expression is rapidly induced upon stimulation through the TCR. Flow cytometric analysis of thymocytes showed that Cybr expression, as measured by GFP, was present at low levels in immature CD69$^{low}$ thymocytes (Fig. 2C). Moreover, in vitro stimulation with anti-CD3 and anti-CD28 showed a marked enhancement of Cybr promoter activity in activated CD69$^+$ thymocytes, which is consistent with its expression pattern during thymic development. Despite the regulated expression of Cybr in the thymus, Cybr$^{-/-}$ mice showed no changes in the thymic ratios of CD4 and CD8 populations or in double-positive or double-negative populations (Fig. 3A). In addition,

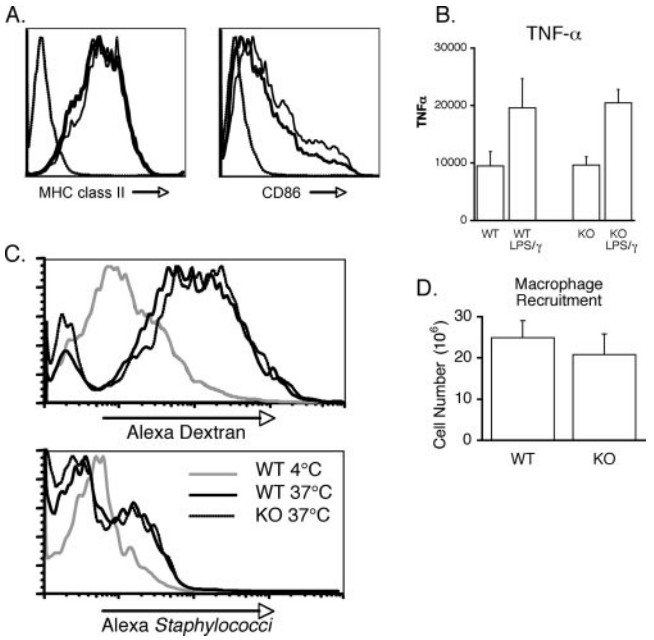


FIG. 6. Normal myeloid cell functions in the absence of Cybr. (A) BMDCs were cultured from wild-type and Cybr-deficient mice and analyzed for the ability to upregulate MHC class II and CD86 by flow cytometry after LPS stimulation. Dashed (leftmost) line, isotype control; solid line, wild type; bold line, Cybr knockout. (B) BMDCs were also tested for their ability to produce cytokines in response to LPS stimulation in vitro. Error bars indicate standard errors of the mean. WT, wild type; KO, knockout. (C) Using Alexa Fluor-labeled dextran or whole bacteria, Cybr-deficient antigen presenting cells were tested for macropinocytosis or phagocytosis. BMDCs were incubated with Alexa dextran at 4 or 37°C for 30 min before being washed and analyzed by flow cytometry (upper panel). Alternatively, activated peritoneal macrophages were incubated with Alexa staphylococci for 30 min, washed, and analyzed by flow cytometry for cell-associated bacteria (bottom panel). Wild-type or *Cybr*$^{-/-}$ mice were injected intraperitoneally with 1 ml of 3% thioglycolate solution, and peritoneal exudate cells were recovered 24 h later. (D) Cells were quantified by counting on a hemacytometer. Error bars indicate standard errors of the mean. WT, wild type; KO, knockout.

there were normal proportions and absolute numbers of CD4$^+$ and CD8$^+$ T cells as well as CD19$^+$ B cells in the spleen (Fig. 3B). Splenic NK cell populations were also normal (data not shown).

**Normal activation of Cybr-deficient T cells.** As Cybr was apparently dispensable for the development of T cells in vivo, we assessed the effects of Cybr deficiency on T-cell functions. To see whether there was a defect early in T-cell activation, we first examined conjugate formation between purified T cells and anti-TCR-coated beads. Conjugate formation was unaltered by Cybr deficiency as was the ability to recruit cytoplasmic proteins, such as phospho-ZAP70 and phospho-LAT, to the immunological synapse (data not shown). In addition, an analysis of the calcium flux in Cybr-deficient T cells showed that early TCR signaling was unaltered (Fig. 4A).

Since no early signaling defects were detected, we next examined effector functions of T cells. One critical aspect of T-cell function is the ability to proliferate and produce cytokines in response to TCR signaling. CD3$^+$ T cells were purified from spleens and lymph nodes of *Cybr*$^{-/-}$ or wild-type mice and cultured on plates coated with increasing concentrations of anti-CD3 in the presence or absence of anti-CD28. We found that Cybr deficiency had no effect on T-cell proliferation or cytokine production (Fig. 4B).

Another important aspect of T-cell function is the differentiation of naïve CD4$^+$ T cells into either T helper 1 (Th1) cells that produce IFN-γ and promote resistance to intracellular pathogens or Th2 cells that produce IL-4 and mediate immunity to helminths. Cybr has previously been shown to be induced by IL-12 and to be a Th1-associated gene in human cells (19). Therefore, we considered the possibility that Th1 differentiation might be disordered. To test the potential of Cybr-deficient T cells to differentiate normally into helper T-cell lineages, we polarized naïve CD4$^+$ T cells under either Th1 or Th2 conditions for 7 days. Cells were then restimulated with plate-bound anti-CD3 for 4 h to detect IFN-γ and IL-4 production. Like the wild-type cells, Cybr-deficient cells grown under Th1 conditions produced IFN-γ mRNA and protein, whereas those grown under Th2 conditions made IL-4 mRNA and protein at wild-type levels (Fig. 4C). Therefore, *Cybr*$^{-/-}$ T cells have the potential to differentiate into either Th1 or Th2 effector cells in the presence of exogenous cytokines. Consistent with normal effector T-cell development, Cybr deficiency also did not alter host survival to infection with the strong Th1-inducing parasite *Toxoplasma gondii* (data not shown), resistance to which requires the activation of CD4 and CD8 cells and the production of IFN-γ.

**Innate immunity in the absence of Cybr.** The initial response of the host to pathogenic microorganisms is through the recognition of pathogen-associated molecular patterns by Toll-like receptors. LPS challenge of mice leads to the signaling through Toll-like receptor 4 and activation of myeloid cells with subsequent production of various proinflammatory cytokines (3). Because Cybr is highly expressed in myeloid cells such as macrophages and dendritic cells, we next assessed the function of these cells in Cybr-deficient mice upon LPS challenge. Innate functions of *Cybr*$^{-/-}$ myeloid cells, as measured by cytokine production in response to LPS challenge, were similar to those in wild-type mice (Fig. 5).

Previous reports have implicated Cybr in DC functions, including migration and adhesion between DC-T conjugates. Therefore, we sought to more rigorously test for defects in myeloid cells. First we examined the generation of BMDCs in vitro. BMDCs could be generated at comparable levels from both wild-type and Cybr-deficient mice in the presence of granulocyte-macrophage colony-stimulating factor and IL-4 (data not shown). These BMDCs expressed similar basal levels of the cell surface markers major histocompatibility complex (MHC) class II, CD80, and CD86 (data not shown), which were upregulated upon LPS stimulation (Fig. 6A). They also produced levels of TNF-α similar to those of wild-type BMDCs in response to stimulation with LPS plus IFN-γ (Fig. 6B), consistent with in vivo results. Cybr-deficient myeloid cells were also assayed for the ability to internalize soluble or particulate antigens. *Cybr*$^{-/-}$ peritoneal macrophages internalized fluorescently labeled antigen (dextran) or whole bacteria and were as efficient as wild-type macrophages at both macropinocytosis and phagocytosis (Fig. 6C).

Since cytohesins have been directly implicated in the regulation of β2 integrin-mediated adhesion, we also tested the ability of these myeloid cells to migrate in vivo. Similar num-

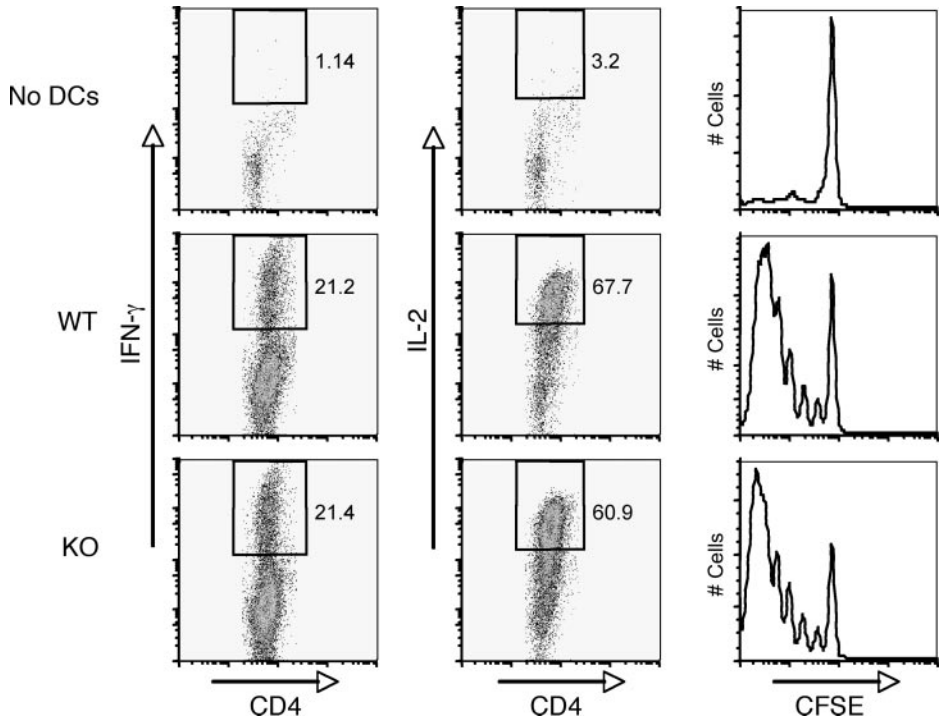


FIG. 7. Cybr-deficient DCs prime T cells in vivo. Wild-type (WT) or *Cybr*$^{-/-}$ BMDCs were pretreated with LPS plus IFN-γ, pulsed with OVA peptide, and analyzed for the ability to prime OVA-specific TCR transgenic T cells in vivo. OVA-pulsed BMDCs were injected into the footpads of CD45.1$^+$ congenic mice. Concomitantly, CD45.2$^+$ CFSE-labeled OT-II T cells were injected into the tail veins of recipient mice. Three days later, draining lymph nodes were isolated and CD45.2$^+$ CD4$^+$ T cells were analyzed for cytokine production by intracellular staining and for proliferation by CFSE dilution. KO, knockout.

bers of activated peritoneal macrophages were elicited from wild-type and Cybr-deficient mice after intraperitoneal injection of thioglycolate, indicating normal recruitment and migration of macrophages (Fig. 6D), which suggests that macrophage migration is not dependent upon the function of Cybr.

To further examine the in vivo functions of Cybr-deficient DCs, BMDCs derived from wild-type or Cybr-deficient mice were pulsed with ovalbumin (OVA) peptide plus IFN-γ and adoptively transferred into CD45.1$^+$ congenic mice that had received CD45.2$^+$ CFSE-labeled OT-II TCR transgenic T cells just prior to the BMDCs. Three days later, donor-derived T cells from draining lymph nodes were analyzed by fluorescence-activated cell sorting (FACS) for proliferation and cytokine production. We did not find any difference between wild-type and Cybr-deficient DCs in antigen presentation to OT-II TCR transgenic T cells in vivo (Fig. 7).

***Cybr*$^{-/-}$ mice have a mild competitive disadvantage in repopulating hematopoietic compartments.** Because we had not observed any developmental or functional defects in hematopoietic cells, we tested the efficiency with which Cybr-deficient stem cells repopulate the hematopoietic compartments of irradiated recipient mice in the presence or absence of competing wild-type stem cells. Equal numbers of lineage-negative c-Kit$^+$ cells from wild-type and *Cybr*$^{-/-}$ mice were injected separately or as a 1:1 mixture into irradiated *rag2*$^{-/-}$ recipient mice. After 8 weeks, mice were euthanized and cells were isolated from thymus, lymph node, and spleen and stained for CD45.2$^+$ (*Cybr*$^{-/-}$) or CD45.1$^+$ (*Cybr*$^{+/+}$) cells. While both wild-type and *Cybr*$^{-/-}$ stem cells could fully reconstitute lymph nodes and spleens in a noncompetitive setting, *Cybr*$^{-/-}$ stem cells displayed a mild competitive disadvantage, especially in the generation of CD8$^+$ T cells, in the presence of wild-type stem cells (Fig. 8A). The generation of splenic B cells and conventional B220$^-$ CD11c$^+$ DCs was also modestly impaired. The defect was more apparent in the periphery, suggesting a possible functional role in the migration of hematopoietic cells to peripheral lymphoid organs. Experiments using GFP expression as a marker for Cybr$^{-/-}$ donor cells showed a similar phenotype (data not shown). Although we saw only a small, yet reproducible, in vitro defect in *Cybr*$^{-/-}$ T-cell chemotaxis in response to the chemokine CXCL12 (data not shown), in vivo homing of isolated, mature Cybr-deficient T cells to the spleens of congenic recipient mice was not impaired compared to wild-type T cells (Fig. 8B). Likewise, we tested whether Cybr knockout DCs displayed a migration defect in vivo by injecting purified CD45.2$^+$ BMDCs generated in vitro from either wild-type or Cybr-deficient bone marrow into the footpads of CD45.1$^+$ congenic mice and monitoring their migration to the draining lymph node after 24 h. Consistent with the T-cell data, the migration of DCs to the draining lymph node was not altered in the *Cybr*$^{-/-}$ cells (Fig. 8C). Therefore, it is likely that Cybr is not affecting stem cell repopulating activity through a role in mature cell migration.

## DISCUSSION

Several lines of evidence have predicted a role for Cybr in T-cell development and functions in vivo. Previous microarray

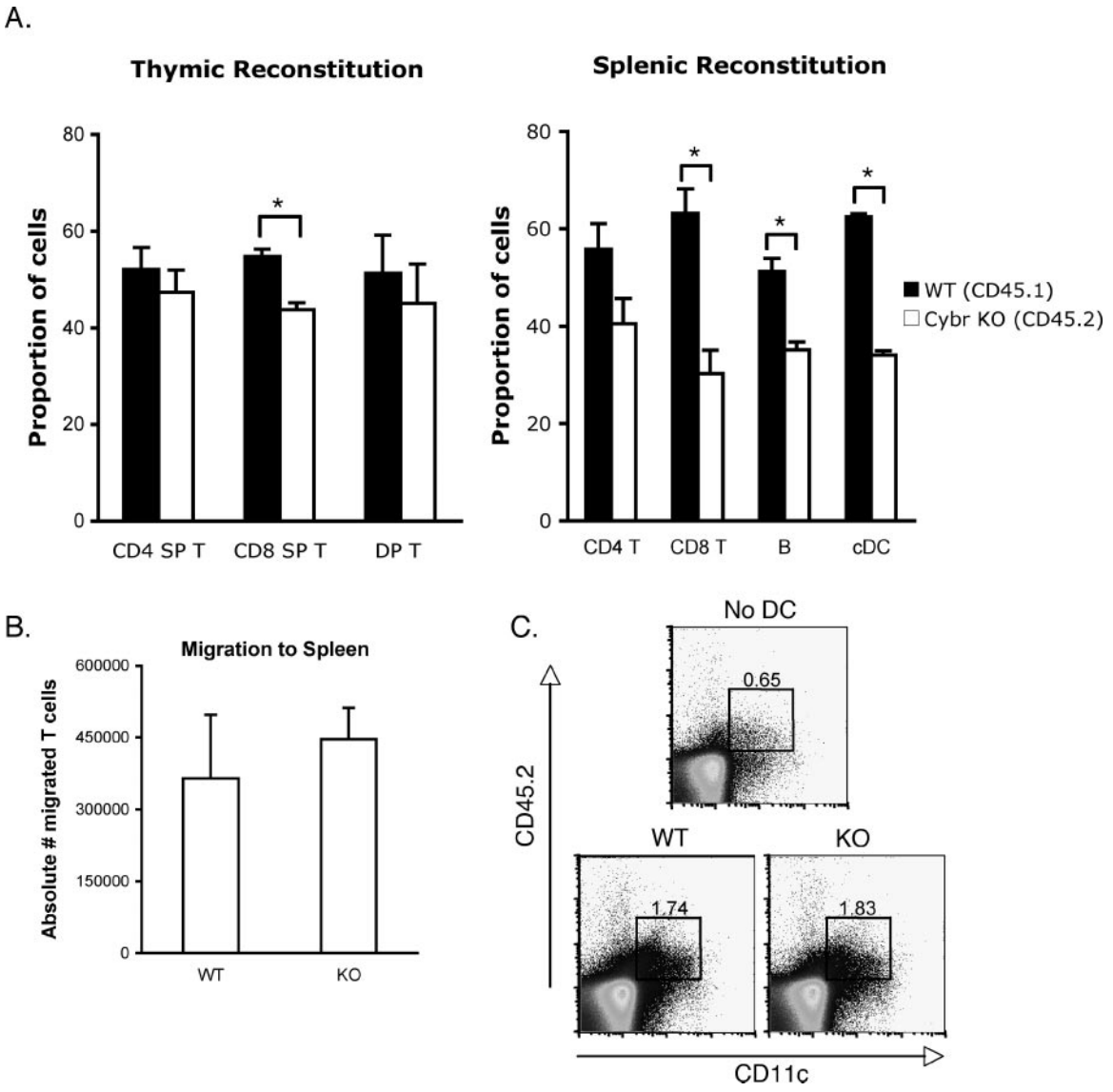


FIG. 8. Cybr$^{-/-}$ hematopoietic stems cells have impaired repopulating activity. (A) Three million purified bone marrow stem cells were injected into the lateral tail veins of irradiated *rag2*$^{-/-}$ recipients, by using all wild-type stem cells (CD45.2$^+$), all Cybr-deficient (CD45.2$^+$) stem cells, or a 1:1 mixture of wild-type (CD45.1$^+$) and Cybr-deficient (CD45.2$^+$) stem cells to produce chimeras. After 8 weeks, thymi, spleens, and lymph nodes were harvested and stained for FACS analysis of T-cell populations. In chimeric mice, CD45.2$^+$ cells represent those that have matured from Cybr knockout stem cells. Error bars indicate standard errors of the mean. Asterisks indicate $P < 0.05$. DP, double positive; SP, single positive; cDC, conventional dendritic cells. (B) Trafficking of wild-type or Cybr-deficient T cells in vivo was analyzed by injecting three million purified CD3$^+$ CD45.2$^+$ T cells intravenously into congenic CD45.2$^+$ recipient mice. Error bars indicate standard errors of the mean. Cell migration was measured by flow cytometry on spleens and lymph nodes 20 h later ($n = 5$ animals per group). (C) In vivo migration of dendritic cells was also assessed. BMDCs were injected into the footpads of mice, and draining lymph nodes were isolated 24 h later. Cells were stained for the appearance of migrating donor-derived dendritic cells within the draining lymph node. WT, wild type; KO, knockout.

studies identified Cybr as a gene regulated during positive selection in the thymus, suggesting a possible role for Cybr in thymocyte development (6, 13). In fact, we show in the present study that Cybr mRNA levels are regulated during thymic development from CD4$^+$ CD8$^+$ cells to the single-positive stages. However, thymic populations were not altered in Cybr-deficient mice. The overexpression of Cybr in Jurkat cells caused a modest, yet reproducible inhibition of cell adhesion to intercellular adhesion molecule 1-treated surfaces (1). Expression data also suggested that Cybr might function in T helper cell differentiation since Cybr mRNA is induced by IL-12 and differentially expressed in human Th1 and Th2 cells. Again, there was no defect in T-cell functions, including proliferation, cytokine secretion, and T helper cell differentiation. In addition, Cybr-deficient mice were no more susceptible to *T. gondii* infection than were wild-type mice, providing further confirmation that Cybr-deficient T-cell functions are relatively normal in vitro and in vivo.

Recently, Cybr has also been implicated in dendritic cell functions, specifically in the association of DCs with T cells, based on overexpression and siRNA studies (5). Despite this report, we now show that mice deficient in Cybr develop nor-

mal dendritic-cell populations with normal responses to antigen stimulation in vivo. In adoptive transfer experiments, DCs must take up antigen, migrate to the lymph nodes, and present antigen in the context of MHC molecules to T cells. None of these functions were impaired in *Cybr*$^{-/-}$ cells since T cells proliferated and secreted cytokines normally in response to *Cybr*$^{-/-}$ DCs (Fig. 7).

The lack of a severe phenotype in *Cybr*$^{-/-}$ mice could be due to redundancy by functionally similar molecules. For example, a protein with high homology to Cybr, named tamalin, has been shown to interact with cytohesins as well. However, the fact that tamalin's expression is restricted to neuronal cells makes it an unlikely candidate for functional redundancy in T and dendritic cells (8, 9). Despite the lack of structural homology, another molecule functionally related to Cybr and tamalin is GRP-1-associated protein (GRSP-1), a retinoic acid-induced cytohesin-binding protein reportedly expressed primarily in mouse brain (16). Analogous to Cybr's association with cytohesin-1, GRSP-1 has been shown to interact with the general receptor for phosphoinositides-1 (GRP-1 or cytohesin-3). Our data suggest even higher levels of GRSP-1 expression in spleen, bone marrow, and lung relative to the expression in brain (see Fig. S1A in the supplemental material). Furthermore, like Cybr, GRSP-1 expression is up-regulated by IL-12 stimulation and is preferentially expressed in Th1 cells (see Fig. S1B in the supplemental material). Therefore, GRSP-1 may be functionally redundant with Cybr in hematopoietic cells. It should also be pointed out that the previous studies of overexpressing Cybr in a T-cell line or interfering with Cybr expression by siRNA employed human cells. Therefore, while we do not favor this possibility, we cannot exclude the possibility that species differences are responsible for the phenotypic disparities observed between our study and the other studies.

Although we did not observe an overt phenotype under normal conditions, an analysis of Cybr-deficient stem cells in a competitive setting showed a defect in the ability of those cells to compete with wild-type cells in repopulating the hematopoietic lineages of irradiated recipient mice. This suggests that there is a contribution of Cybr to the engraftment of bone marrow stem cells. The precise role Cybr plays in bone marrow reconstitution is unknown but may be related to cell migration. CXCL12 has been implicated in directing the trafficking of lymphocytes, monocytes, and hematopoietic stem cells between niches (10). Lethally irradiated mice reconstituted with fetal liver cells lacking the gene encoding the CXCL12 receptor CXCR4 have increased lymphoid precursors in the blood, with corresponding decreases in the bone marrow (11). In vivo trafficking of mature T cells and dendritic cells (which depends primarily upon CCR7 ligands) to lymphoid organs was not altered by Cybr deficiency. Therefore, we believe that either stem cell migration itself is preferentially affected compared to mature cell trafficking or stem cell lineage commitment/differentiation may be impaired. The precise contributions of Cybr to cell trafficking versus differentiation remain to be determined. It is clear, however, that the reported role for Cybr in hematopoietic cell adhesion and cell-cell contact is not as significant as predicted by previously published results based on protein overexpression and in vitro assays.

## ACKNOWLEDGMENTS

This research was supported by the Intramural Research Program of the NIH, National Institute of Arthritis and Musculoskeletal and Skin Diseases.

We thank Alan Sher and Dragana Jankovic for the infection of Cybr-deficient mice with *T. gondii*.

## REFERENCES

1. **Boehm, T., S. Hofer, P. Winklehner, B. Kellersch, C. Geiger, A. Trockenbacher, S. Neyer, H. Fiegl, S. Ebner, L. Ivarsson, R. Schneider, E. Kremmer, C. Heufler, and W. Kolanus.** 2003. Attenuation of cell adhesion in lymphocytes is regulated by CYTIP, a protein which mediates signal complex sequestration. EMBO J. **22:**1014–1024.
2. **Cogliati, T., D. J. Good, M. Haigney, P. Delgado-Romero, M. A. Eckhaus, W. J. Koch, and I. R. Kirsch.** 2002. Predisposition to arrhythmia and autonomic dysfunction in Nhlh1-deficient mice. Mol. Cell. Biol. **22:**4977–4983.
3. **Downey, J. S., and J. Han.** 1998. Cellular activation mechanisms in septic shock. Front. Biosci. **3:**d468–d476.
4. **Geiger, C., W. Nagel, T. Boehm, Y. van Kooyk, C. G. Figdor, E. Kremmer, N. Hogg, L. Zeitlmann, H. Dierks, K. S. Weber, and W. Kolanus.** 2000. Cytohesin-1 regulates beta-2 integrin-mediated adhesion through both ARF-GEF function and interaction with LFA-1. EMBO J. **19:**2525–2536.
5. **Hofer, S., K. Pfeil, H. Niederegger, S. Ebner, V. A. Nguyen, E. Kremmer, M. Auffinger, S. Neyer, C. Furhapter, and C. Heufler.** 2005. Dendritic cells regulate T-cell deattachment through the integrin-interacting protein CYTIP. Blood **7:**1003–1009.
6. **Huang, Y. H., D. Li, A. Winoto, and E. A. Robey.** 2004. Distinct transcriptional programs in thymocytes responding to T cell receptor, Notch, and positive selection signals. Proc. Natl. Acad. Sci. USA **101:**4936–4941.
7. **Jackson, T. R., B. G. Kearns, and A. B. Theibert.** 2000. Cytohesins and centaurins: mediators of PI 3-kinase-regulated Arf signaling. Trends Biochem. Sci. **25:**489–495.
8. **Kitano, J., K. Kimura, Y. Yamazaki, T. Soda, R. Shigemoto, Y. Nakajima, and S. Nakanishi.** 2002. Tamalin, a PDZ domain-containing protein, links a protein complex formation of group 1 metabotropic glutamate receptors and the guanine nucleotide exchange factor cytohesins. J. Neurosci. **22:**1280–1289.
9. **Kitano, J., Y. Yamazaki, K. Kimura, T. Masukado, Y. Nakajima, and S. Nakanishi.** 2003. Tamalin is a scaffold protein that interacts with multiple neuronal proteins in distinct modes of protein-protein association. J. Biol. Chem. **278:**14762–14768.
10. **Lazarini, F., T. N. Tham, P. Casanova, F. Arenzana-Seisdedos, and M. Dubois-Dalcq.** 2003. Role of the alpha-chemokine stromal cell-derived factor (SDF-1) in the developing and mature central nervous system. Glia **42:**139–148.
11. **Ma, Q., D. Jones, and T. A. Springer.** 1999. The chemokine receptor CXCR4 is required for the retention of B lineage and granulocytic precursors within the bone marrow microenvironment. Immunity **10:**463–471.
12. **Mansour, M., S. Y. Lee, and B. Pohajdak.** 2002. The N-terminal coiled coil domain of the cytohesin/ARNO family of guanine nucleotide exchange factors interacts with the scaffolding protein CASP. J. Biol. Chem. **277:**32302–32309.
13. **Mick, V. E., T. K. Starr, T. M. McCaughtry, L. K. McNeil, and K. A. Hogquist.** 2004. The regulated expression of a diverse set of genes during thymocyte positive selection in vivo. J. Immunol. **173:**5434–5444.
14. **Moriguchi, M., B. D. Hissong, M. Gadina, K. Yamaoka, H. L. Tiffany, P. M. Murphy, F. Candotti, and J. J. O'Shea.** 2005. CXCL12 signaling is independent of Jak2 and Jak3. J. Biol. Chem. **280:**17408–17414.
15. **Morinobu, A., M. Gadina, W. Strober, R. Visconti, A. Fornace, C. Montagna, G. M. Feldman, R. Nishikomori, and J. J. O'Shea.** 2002. STAT4 serine phosphorylation is critical for IL-12-induced IFN-γ production but not for cell proliferation. Proc. Natl. Acad. Sci. USA **99:**12281–12286.
16. **Nevrivy, D. J., V. J. Peterson, D. Avram, J. E. Ishmael, S. G. Hansen, P. Dowell, D. E. Hruby, M. I. Dawson, and M. Leid.** 2000. Interaction of GRASP, a protein encoded by a novel retinoic acid-induced gene, with members of the cytohesin family of guanine nucleotide exchange factors. J. Biol. Chem. **275:**16827–16836.
17. **Randazzo, P. A., Z. Nie, K. Miura, and V. W. Hsu.** 2000. Molecular aspects of the cellular activities of ADP-ribosylation factors. Sci. STKE **2000:**RE1.
18. **Rogge, L., E. Bianchi, M. Biffi, E. Bono, S. Y. Chang, H. Alexander, C. Santini, G. Ferrari, L. Sinigaglia, M. Seiler, M. Neeb, J. Mous, F. Sinigaglia, and U. Certa.** 2000. Transcript imaging of the development of human T helper cells using oligonucleotide arrays. Nat. Genet. **25:**96–101.
19. **Tang, P., T. P. Cheng, D. Agnello, C. Y. Wu, B. D. Hissong, W. T. Watford, H. J. Ahn, J. Galon, J. Moss, M. Vaughan, J. J. O'Shea, and M. Gadina.** 2002. Cybr, a cytokine-inducible protein that binds cytohesin-1 and regulates its activity. Proc. Natl. Acad. Sci. USA **99:**2625–2629.
20. **Yamaoka, K., B. Min, Y. J. Zhou, W. E. Paul, and J. O'Shea, J.** 2005. Jak3 negatively regulates dendritic-cell cytokine production and survival. Blood **106:**3227–3233.